HHS Public Access

Author manuscript

Annu Rev Virol. Author manuscript; available in PMC 2017 September 29.

Published in final edited form as:

Annu Rev Virol. 2016 September 29; 3(1): 555–572. doi:10.1146/annurev-virology-110615-042249.

Modeling Viral Spread

Frederik Graw[1] and **Alan S. Perelson**[2]

Alan S. Perelson: asp@lanl.gov

[1]Center for Modelling and Simulation in the Biosciences, BioQuant Center, Heidelberg University, 69120 Heidelberg, Germany

[2]Theoretical Biology and Biophysics, Los Alamos National Laboratory, Los Alamos, New Mexico 87545

Abstract

The way in which a viral infection spreads within a host is a complex process that is not well understood. Different viruses, such as human immunodeficiency virus type 1 and hepatitis C virus, have evolved different strategies, including direct cell-to-cell transmission and cell-free transmission, to spread within a host. To what extent these two modes of transmission are exploited in vivo is still unknown. Mathematical modeling has been an essential tool to get a better systematic and quantitative understanding of viral processes that are difficult to discern through strictly experimental approaches. In this review, we discuss recent attempts that combine experimental data and mathematical modeling in order to determine and quantify viral transmission modes. We also discuss the current challenges for a systems-level understanding of viral spread, and we highlight the promises and challenges that novel experimental techniques and data will bring to the field.

Keywords

HIV; HCV; cell-to-cell infection; cell-free virus infection; mathematical modeling; agent-based models

INTRODUCTION

There are an estimated 10^{31} different viruses on Earth (1) that have each evolved strategies to invade a host and establish infection. After an infectious viral particle has crossed the first barrier of a host (e.g., skin, epithelial tissue), its ability to successfully spread within a tissue depends on finding appropriate target cells in which to efficiently replicate and transmit viral progeny, and on bypassing or modulating counteracting host responses.

Virus particles represent efficiently structured pathogens mainly consisting of viral genetic material and a protective coat. They need to enter host cells and hijack their molecular machinery in order to replicate. To cross the cellular membrane, different viruses have found

DISCLOSURE STATEMENT

The authors are not aware of any affiliations, memberships, funding, or financial holdings that might be perceived as affecting the objectivity of this review.

different strategies, sometimes involving the complex interaction of several cell surface receptors: For example, in human immunodeficiency virus type 1 (HIV-1) infection, viral glycoproteins on the viral envelope interact with the cell surface proteins CD4 and the CCR5 or CXCR4 receptor on T lymphocytes to mediate viral entry (2). For hepatitis C virus (HCV), a cascade of receptor interactions is needed for infection of hepatocytes. This cascade starts with the virus interacting with scavenger receptor class B type I (SR-BI) (3) and then tetraspanin CD81 (4), which forms complexes with the tight junction proteins claudin 1 and/or occludin and the Niemann-Pick C1–like 1 (NPC1L1) receptor (5–7). For hepatitis B virus and hepatitis D virus, the human sodium/taurocholate cotransporting polypeptide (hNTCP) and glypican 5 have recently been identified as required host entry factors (8, 9). Other viruses use other host cell receptors. Interestingly, some pathogens, such as HIV-1 and HCV, have found ways to vary their receptor dependencies by using alternative receptors or alternative entry pathways in parallel (10, 11).

The interactions of virion surface proteins with cell surface molecules characterize cell-free viral transmission events. Although cell-free transmission strategies enhance viral spread by allowing diffusing virions to infect distant cells, they also have some disadvantages, as freely diffusing virions can be subject to antibody neutralization as well as antibody-mediated opsonization and phagocytosis (12–14).

Direct cell-to-cell transmission of intact virions or viral genetic material is another means of transmitting viral infection and involves contacts between infected and uninfected cells. Many viruses that are pathogenic for humans, including HIV-1 and HCV, are capable of spreading by cell-to-cell transmission (15, 16). Several mechanisms of cell-to-cell spread have been described, including membrane fusion, the formation of virological synapses, the use of tight junction proteins, and the formation of long-ranging nanotubes (reviewed in 15, 17). Although cell-free transmission via diffusing virions is important for the initialization of infection, cell-to-cell transmission seems to be much more potent in mediating viral spread; for example, for HIV-1, the efficiency of spread is estimated at 10-fold to 18,000-fold greater for cell-to-cell transmission than for cell-free infection (18–20). The robustness of transmission of infection, the shielding of viral particles from neutralizing antibodies and phagocytosis, and the ability to transmit multiple viral genomes contribute to this greater efficiency. Some estimates in the literature suggest that as many as 10^2–10^3 virions can be simultaneously transmitted through a single synapse (18, 21).

Due to this high multiplicity of infection, Sigal et al. (12) argued that antiretroviral agents that act intracellularly, such as the reverse transcriptase inhibitor tenofovir, should have reduced activity in blocking cell-to-cell infection, and they verified this hypothesis in vitro. For a simple argument as to why one might expect this to be true, consider a situation in which a single virion has a probability p of infecting a cell. Then, assuming virions act independently, if n virions enter a cell, the probability that at least one of them successfully infects is $P_I = 1 - (1 - p)^n$. To be more explicit, if $p = 0.1$, then with one virion entering the probability of infection is 10% and with 100 virions entering the probability is 0.99997, that is, ~100%. Now consider a drug that is 95% effective. In the case of one virion entering, the probability of infection in the presence of the drug is reduced to $p = 0.1 \times 0.05 = 0.005$. For the case of 100 virions, with p now equal to 0.005, the probability that at least one virion

succeeds in infecting the cell is then $P_1 = 0.39$. Rather than reducing the probability of infection by 95%, as in the case of an infection by a single virion, the drug reduces the probability of infection by only 61% when 100 virions are transmitted during the infection of a single cell, as might occur during cell-to-cell transmission. Despite this simple argument, Agosto et al. (22, 23) later showed that most nonnucleoside reverse transcriptase inhibitors, protease inhibitors, and entry inhibitors remain highly effective even when infection is cell-to-cell, suggesting the mechanism of action of the drug and its target are important factors. Further, the assumption that each virion has the same probability of infecting a cell when transmission is by cell-free virions or cell-to-cell infection may not be valid (24). Whether drugs are less effective or not, the properties of robustness, multiple genome transmission, and immune evasion could explain why cell-to-cell spread seems to be an important mechanism for the establishment and maintenance of persistent infections (12, 14, 25).

Recently, it has been shown that the transfer of HIV-1 genetic material by cell-to-cell transmission into resting $CD4^+$ T cells can trigger pyroptotic death (26). Death is due to an innate immune response against incomplete cytosolic viral DNA intermediates that accumulate in these cells. Cell-free HIV-1 virions, even when added in large quantities, fail to activate this death pathway, highlighting an important role of cell-to-cell transmission in HIV pathogenesis (26).

As cell-to-cell transmission predominantly occurs in solid tissues, it has been difficult to distinguish between cell-to-cell and cell-free virus transmission modes, and the extent to which different viruses exploit these modes of spread in vivo is unknown. In such circumstances, mathematical models may be informative.

Mathematical models have been an essential tool in determining the dynamics of viral infections based on experimental and clinical data (27). They allow one to examine the dynamics of viral replication and spread in vivo and in vitro within a systematic and quantitative framework. Analyzing experimental and clinical data with mathematical models has helped to quantify the in vivo rate of HIV-1 and HCV viral replication (28–30) and the clearance rate of virions and infected cells in both HIV-1 (28, 31) and HCV infection (30, 32) and to determine how specific drugs mediate their antiviral efficacy (30, 32–35). Further, mathematical models allow the quantification of processes that are hidden within the data and that cannot be measured and/or observed directly.

Below, we discuss how mathematical models have been used to quantify viral spread and to determine the extent to which viruses, such as HIV-1 and HCV, exploit cell-to-cell spread in vivo. We review different ways in which the processes of viral spread have been modeled and discuss the way these models have been applied to experimental data. In addition, we highlight recent developments in experimental techniques that will improve our understanding of viral spread mechanisms in vitro and in vivo, and we describe how they can be used for the quantification of these processes. We also outline the challenges that still need to be resolved in order to fully determine how HIV-1 and HCV infections spread in vivo.

MODELING CELL-TO-CELL TRANSMISSION FOR HIV-1

Modes of Viral Transmission and Modeling Viral Dynamics

The well-known standard model of viral dynamics (reviewed in 27, 36) represents the dominant and standard approach to analyze and quantify the spread of a viral infection within a host. The model follows the concentrations of target cells (T), infected cells (I), and virions (V). Their interactions, depicted in **Figure 1*a***, are mathematically described by the following system of ordinary differential equations:

$$\begin{aligned} \mathrm{d}T/\mathrm{d}t &= \lambda - \beta VT - \omega IT - \mathrm{d}_T T \\ \mathrm{d}I/\mathrm{d}t &= \beta VT + \omega IT - \delta I \\ \mathrm{d}V/\mathrm{d}t &= \rho I - cV. \end{aligned} \qquad 1$$

Target cells, T, which are cells susceptible to infection, are produced at a constant rate λ and have an average lifetime of $1/\mathrm{d}_T$. Infected cells, I, die with rate δ per cell and produce new virions at rate ρ that are cleared from the system at rate c per virion. In the formulation given in Equation 1, infection of target cells is mediated (*a*) by cell-free virions at a rate dependent on the viral concentration, V, and a transmission rate constant β and (*b*) by infected cells with a cell-to-cell transmission rate constant ω. When cell-to-cell transmission is included in the model, virus spread and target cell depletion are accelerated (**Figure 1*b***).

Whereas most previous analyses used the standard model of viral dynamics based on the assumption that infection is solely transmitted by cell-free virions (ω = 0) (27, 30, 33, 37, 38), recent models have incorporated cell-to-cell transmission by allowing both modes of transmission within the model (β ≠ 0, ω ≠ 0) (39–42). Iwami et al. (42) used a model as shown in Equation 1 to analyze the contribution of cell-to-cell transmission to HIV-1 spread in vitro by comparing static and shaking culture systems. The shaking of the culture is assumed to inhibit the formation of cell-to-cell contacts (20) and thus to prevent cell-to-cell transmission (ω = 0), whereas the static culture system allows for both modes of transmission. Fitting the model to time course data on the number of infected and uninfected cells and the viral load in the static and shaking culture systems simultaneously to estimate the kinetic parameters, they found that cell-to-cell transmission was responsible for ~60% of the viral spread. Thus, cell-to-cell transmission seems to be the predominant mode of spread for HIV-1 in vitro. In a different in vitro system using fluorescent virus transfer, Chen et al. (18) also concluded that cell-to-cell transfer is the dominant mechanism of HIV-1 transmission. In vivo, experiments on acute HIV-1 transmission in humanized mice indicated that migration of infected cells, and not solely viral diffusion, is necessary to promote systemic viral spread (43). Further, in an analysis of the distribution of multiple HIV-1 proviruses present in HIV-infected $CD4^+$ T cells taken from the spleens of two infected individuals, Dixit & Perelson (44) estimated that ~10% of infections in lymphoid tissue are mediated by cell-free virions, whereas 90% occur via cell-to-cell transfer.

Zhang et al. (39) used an extended version of the model depicted in Equation 1 to analyze viral progression in treatment-naive HIV-1-infected patients. They distinguished between quiescent and activated uninfected cells as well as latently infected cells. In contrast to

Iwami et al. (42), Zhang et al. (39) used parameters from the literature to study the ability of the model to reproduce clinical data, focusing on the contribution of the different modes of viral spread. They found that both modes of HIV-1 transmission are essential for the establishment and persistence of the infection, but that cell-to-cell transmission is important for disease progression and becomes dominant during the late phases of the infection. Although their model could reproduce viral load and $CD4^+$ T cell count changes in a cohort of patients, their conclusions about the relative importance of the two mechanisms of spread may be dependent on their choice of parameter values to describe the two modes of transmission. Nonetheless, their results support the current understanding that cell-to-cell transmission is an important mechanism used by viruses to establish persistence.

The Virological Synapse

For HIV-1, the spread of infection by direct cell-cell contacts is facilitated by specific structures called virological synapses (17, 18, 21, 45–47). A single infected cell can form virological synapses with multiple target cells, called polysynapses, and thereby simultaneously infect them (48). The formation of a virological synapse between an infected and an uninfected cell is characterized by an initial adhesion between the cells triggered by an interaction between HIV-1 envelope proteins on the infected cell and CD4 receptors on uninfected $CD4^+$ T cells. This is followed by stabilizing interactions involving cellular adhesion molecules, such as lymphocyte function–associated antigen 1 (LFA-1) and intercellular adhesion molecule 1 (ICAM-1) (47). Confocal microscopy and time-lapse imaging of virological synapse formation have indicated rapid viral assembly at the points of cell-cell contact after cellular adhesion (21). On an artificial membrane containing ICAM-1, addition of HIV-1 envelope protein is sufficient to trigger the arrest of $CD4^+$ T cell migration and the initiation of virological synapse formation (49). Generally, a virological synapse lasts between 10 min and a few hours in vitro (18, 19, 49). During the time the virological synapse exists, infectious viral material is efficiently transmitted between cells (18, 19, 49). Synapses that efficiently transmit infection can also form between virus-carrying dendritic cells and $CD4^+$ T cells (50, 51).

In Equation 1, the kinetics of the processes underlying viral entry, for either cell-to-cell or cell-free transmission, are incorporated within the corresponding transmission rates (i.e., ω and β, respectively). Work has been done on quantifying the number of HIV-1 envelope glycoprotein trimers that need to interact with target cell receptors in order to facilitate virion entry in the case of cell-free infection and its relationship to viral infectivity (reviewed in 52), but corresponding quantitative analysis for virological synapse formation remains rudimentary. Some estimates indicate that roughly ~56% of cell-cell contacts lead to virological synapse formation (21, 46), with only ~0.19 of these synapses leading to a successful infection (18, 20, 53). Consideration of the processes characterizing contact formation will be helpful when trying to quantify the rates of cell-to-cell transmission in comparison to the rates of cell-free transmission. Such an endeavor would help to improve current estimates (39, 42) and to validate their appropriateness.

Multiple Infections

Because multiple viral particles can be transferred simultaneously via a single virological synapse (15, 21, 54), it is plausible that cells infected by cell-to-cell transmission contain multiple integrated proviruses. As mentioned above, infected $CD4^+$ T cells isolated from the spleens of two HIV-1-infected individuals were observed to contain on average 3–4 proviral copies of HIV-1, with some cells having as many as 8 proviruses (55). Because one virion leads to production and integration of at most one provirus, this number suggests that on average at least 3–4 virions entered the cell if the mode of transmission was via cell-free virus. However, the distribution of proviral copy number was bimodal, with peaks at 1 copy and 3 copies per cell. As the spleen is a densely packed organ, allowing frequent cell-cell interactions, the multiple integrated proviruses could also have derived from a single or multiple cell-to-cell transmission events. In contrast, in a study in which cells in blood were analyzed, the vast majority had only a single proviral copy (56), presumably due to inhibition of stable synapse formation by frequent cell mixing (20). Using mathematical models, Dixit & Perelson (44) analyzed the distribution of proviral genomes found in the spleen (55) in order to better understand the mechanisms leading to the observed distribution of multiple infections. In one model they assumed that infections were sequential and that an infected cell containing one provirus could be infected m more times, where m is given by a Poisson distribution. They also accounted for the fact that after infection CD4 is downregulated, making subsequent infections more unlikely (57). This model fit the data with a mean value of m of 2.3 but gave rise to a single-peaked distribution. To explain the bimodal distribution they assumed that infections could occur simultaneously either by cell-free or cell-to-cell transmissions. The best fit of this model to the data suggested that about 90% of infections were by cell-to-cell transmission, with every cell-to-cell event leading on average to the transmission of ~3.4 genomes. This model explained the observed bimodal distribution of proviral copy numbers.

Experiments in vitro by Del Portillo et al. (53) using T cells coexpressing different fluorescent HIV-1 variants showed that multiple HIV-1 genomes could be transmitted across a single virological synapse. The experiments also indicated that, whereas cell-free transmission followed Poisson statistics, cell-associated HIV-1 transmission led to larger numbers of successful viral integrations than predicted by a Poisson distribution, consistent with multiple viral genomes being successfully transmitted through a virological synapse (53). A computational model that followed the fate of individual cells (an agent-based model) in which cells are allowed to interact, form synapses, and transmit infection supported these observations. Further, they also measured on average 3.82 (± 0.56 SEM) proviral copies in cells infected by cell-to-cell contact and 1.3 (± 0.16 SEM) in the case of cell-free infection (53), values that are comparable to observations in vivo (55, 56).

To determine the advantage of multiple infections, Komarova & Wodarz (41) developed a mathematical model describing synaptic transmission. They distinguished between cells infected by i virions, x_i, with $0 \leq i \leq N$, where i is defined as the multiplicity of infection. Here, x_0 is the number of uninfected cells and N the maximal number of virions that can successfully infect a cell—that is, the model assumed that up to N viral genomes can be incorporated into a single cell's genome. Actual synaptic transmission was then modeled by

a mass-action relationship of infected and uninfected cells with a parameter $\gamma^{(m)}_j$ defining the probability of a cell infected with m virions to transmit j virions per synapse (41). The probability $\gamma^{(m)}_j$ contained all information on viral replication and synapse formation in the model. Varying the number of virions transmitted per synapse and the kinetics of synapse formation and viral replication, the authors used their model to compare different viral strategies with regard to their success in maximizing viral spread. Here, by a viral strategy, the authors meant the probability distribution for the number of virions transmitted to a cell by cell-to-cell transmission. For example, one type of strategy would be to always pass on the same mean number of virions, s. Different strategies would correspond to different values of s. Their model is very flexible and allows one to study questions such as what the effects are of assuming the number of virions transmitted depends on the cell's multiplicity of infection or whether the lifetime of an infected cell depends on its multiplicity of infection. Interestingly, they showed that there are circumstances in which transmitting intermediate numbers of virions yields the highest basic reproductive number and hence the highest probability of establishing persistent infection. Komarova et al. (24) used the same model to argue that the decreased drug efficacy of the nucleotide reverse transcriptase inhibitor tenofovir against HIV-1 in vitro observed by Sigal et al. (12) can be due to multiplicity of infection only if multiple transmission—i.e., cell-to-cell transmission—is more efficient than single infection, as in the case of cell-free infection (24).

The advantage of a high multiplicity of infection identified by kinetic and probabilistic arguments was made without considering viral diversity. The transmission of several independent mutant proviral copies into a single cell offers the possibility to increase viral fitness by increasing viral diversity, allowing selection on the quasispecies level (53). Although the number of copies transferred via a single synapse can be on the order of thousands of genomes (18, 21), the number of successfully replicated genomes is usually rather small, ~4–5 (55). Miyashita et al. (58) showed by an integrative analysis of computational simulations and experimental data that the number of viral genomes establishing infection per cell and the number of viral progeny per founder sequence are subject to stochastic variation. This heterogeneity on a cellular and viral level during the whole infection process allows rapid adaptation of the virus to its environment. Observations made for tomato mosaic virus—a positive-strand RNA plant virus—in vivo show how a small number of viral genomes selected for replication upon cell-to-cell transmission of larger viral populations can be advantageous for viral spread (59).

MODELING CELL-FREE AND CELL-TO-CELL TRANSMISSION IN HCV INFECTION

Similar to HIV-1, HCV is able to spread via cell-free diffusing virions and direct cell-to-cell contact (15). However, differences in the characteristics of the main target cell populations require different modeling approaches when trying to analyze viral spread, especially when addressing cell-to-cell transmission.

Modeling Cell-Free Viral Spread and Antiviral Therapy

The standard model of viral infection when applied to HCV infection by cell-free virus and treatment with antiviral drugs, such as interferon-α (IFN) or the current panoply of direct-acting antivirals, takes the following form:

$$\begin{aligned} \mathrm{d}T/\mathrm{d}t &= \lambda - \beta VT - \mathrm{d}_T T \\ \mathrm{d}I/\mathrm{d}t &= \beta VT - \delta I \\ \mathrm{d}V/\mathrm{d}t &= (1-\rho)\varepsilon I - cV, \end{aligned} \qquad 2$$

where ε is the drug effectiveness in blocking viral production, with ε = 1 corresponding to a 100% effective drug. The vast majority of antivirals used for treating HCV infection act by blocking viral replication and/or viral assembly and hence reduce viral production from infected cells. Neumann et al. (30) introduced this model in order to understand the very rapid decay of plasma HCV RNA observed during the first one to two days after the initiation of IFN treatment, when viral levels fell one to two orders of magnitude in a dose-dependent manner. Because hepatocytes are long-lived cells, Neumann et al. assumed that during the first two days of therapy the number of target cells and the number of infected cells remained constant. Further, it had been observed that in untreated chronically infected HCV patients the viral load, measured in terms of HCV RNA copies per milliliter of serum or plasma, remained approximately constant on timescales of days, weeks, and even months. When this occurs, clinicians say the virus has reached a set point. Under these circumstances, the rate of viral production, ρI_0, must equal the rate of viral clearance, cV_0, where the subscript 0 is used to denote baseline or pretherapy value. If therapy is applied at time 0, then the equation for the change in viral load becomes

$$\mathrm{d}V/\mathrm{d}t = (1-\varepsilon)\rho I_0 - cV = (1-\varepsilon)cV_0 - cV,$$

where we have assumed the infected cell level remains constant at its pretherapy value.

When this equation is solved, it predicts that the viral load during therapy will change according to the equation (30)

$$V(t) = V_0\{1 - \varepsilon + \varepsilon \exp[-c(t - t_0)]\},$$

where t_0 represents a pharmacological delay, as IFN needs to bind to its receptor and cause the expression of a large number of IFN-stimulated genes, which in turn affect viral production through complex and not fully understood mechanisms. This equation fit the clinical data taken over the first two days of therapy from a variety of patients extremely well (30). By fitting this equation to the data, both the effectiveness of therapy, ε, and the rate constant for viral clearance, c, could be estimated. Standard IFN given at a dose of 5 million IU day^{-1} was found to be about 80% effective (30). By comparison, applying the theory to modern drugs, such as the HCV polymerase inhibitor sofosbuvir, a Gilead drug that costs $1,000 per pill, showed that sofosbuvir was 99.96% effective (60). This theory

suggested that the in vivo effectiveness of new HCV drugs could be evaluated in very short-term clinical trials, and it was an approach embraced by the pharmaceutical industry.

Also, recall that at the pretherapy viral set point, cV_0, the rate of viral clearance is equal to the rate of viral production. Using the estimate of c and the measured baseline viral loads and adjusting for the total body volume through which virus could be distributed, Neumann et al. (30) concluded that approximately 10^{12} virions are produced and cleared daily. Combining this virion production rate with estimates of the per base error rate of the HCV polymerase (61), Rong et al. (62) later showed that in a person chronically infected with a predominant virus, virions containing HCV RNA with all possible single- and double-mutant variants are likely made every day; this finding highlighted the need for combination therapy to treat HCV infection, as is now becoming commonplace (63). One recent proof-of-concept clinical trial showed that it was possible with response guided therapy to cure a group of HCV genotype 1b chronically infected patients using a combination of an HCV protease inhibitor, a polymerase inhibitor, and an NS5A inhibitor given for only three weeks (64).

Accounting for Spatial Dynamics

The standard model for viral dynamics with the extension for cell-to-cell transmission (Equation 1) does not contain any spatial information and assumes any two cells can interact and form a virological synapse. This assumption is not appropriate for cell-to-cell transmission among stationary cells, such as hepatocytes in the liver. As transmission by cell-to-cell contact allows transmission from infected cells only to their direct neighbors, infections can get trapped in certain areas (65–67), and the speed of progression of infection can be limited due to the lack of target cells in certain locations. Through simulation of viral spread by the standard model of viral dynamics within a spatially defined setting, it was shown that overall infection dynamics are altered, and that models not accounting for spatial aspects might underestimate the true infection dynamics (68). HCV predominantly spreads among hepatocytes, which are epithelial cells that form tight junctions with their neighbors and are spatially organized within the liver. These aspects have to be considered when analyzing and quantifying HCV spread.

Mathematically, infection dynamics in space and time can be modeled by partial differential equations (69–71). Handling such model systems is much more challenging, and these models have rarely been used in analyses of viral dynamics. With recent advances in experimental and imaging techniques (11, 72–74), as well as in computational power, approaches following and simulating the behavior of single cells during an infection have become standard tools of viral dynamics analysis (65). Models that follow the fate of individual cells in space and time have been called agent-based models (65). These models can also include intracellular processes, such as viral replication and viral export from infected cells. Because of their complexity in representing multiple aspects of cellular behavior, they require an increased amount of experimental information to appropriately parameterize the model. Slowly, this type of information is becoming available (75, 76).

Quantifying HCV Cell-to-Cell Spread

Much like for HIV-1, the extent to which HCV exploits cell-free and cell-to-cell transmission in vivo is unknown. Further, the kinetics of HCV cell-to-cell transmission still need to be determined. In combination with experimental data, agent-based models have been used to analyze and quantify the spread of HCV in vivo and in vitro. Using single-cell laser capture microdissection, Kandathil et al. (72) analyzed the infection status of single cells within 2D slices of liver biopsy samples taken from HCV-infected patients and quantified the amount of intracellular viral RNA (vRNA). Plotting the amount of vRNA above a grid representing a set of adjacent cells gives rise to a viral infection landscape, or viroscape (72). Examining sets of viroscapes showed that infected cells tend to occur in small clusters, with individual clusters comprising ~4–50 infected cells (72). Such clustered landscapes are consistent with the hypothesis that HCV exploits both cell-free and cell-to-cell modes of transmission in vivo, with isolated clusters being founded by cell-free infection and then growing by local spread. The local spread can be due to cell-to-cell transmission or to the preferential infection of neighboring cells when virions are released from an infected cell. In addition, analyzing Kandathil et al.'s data in more detail, Graw et al. (77) found that the amount of intracellular HCV RNA declines from the cell with the highest level of vRNA, which presumably founded the cluster, to cells at the outer boundary of the cluster. Similar observations of HCV foci in tissue samples have been made by others (73, 78, 79). Determining whether the local spread and the observed patterns are largely dependent on cell-to-cell transmission is difficult— experimentally and theoretically—and may be possible only if both modes of transmission have vastly differing kinetics.

Two different approaches have been used to determine the rate at which cell-to-cell transmission occurs during HCV infection.

Analyzing focus spread in vitro—Studying HCV spread in vitro allows one to control viral transmission modes to a certain extent. Administration of antibodies against the HCV envelope protein E2 blocks HCV spread by cell-free virions in vitro (7). Viral spread in the presence of anti-E2 treatment is characterized by the growth of existing foci and thus is mostly driven by direct cell-to-cell transmission. In addition, the proliferation of infected cells, which can also be viewed as a form of cell-to-cell transmission, may also play a role. In order to quantify HCV cell-to-cell transmission, Graw et al. (80) described focus growth as a stochastic process. A number of different models of viral spread were examined to estimate focus growth rates. In one it was assumed that each infected cell in a focus can infect another cell at a constant rate ρ in the absence of cell-free virus transmission. This model worked well in describing the growth rate of small clusters, where neighboring target cells are plentiful. To explain the growth kinetics of larger foci, Graw et al. assumed that foci grow radially and only infected cells at the perimeter of a focus contribute to focus growth. Using this model to explain data collected in vitro in a system using Huh7 cells infected by JFH-1 virions they estimated a focus growth rate of $\rho \approx 3 \times 10^{-2}$ to 7×10^{-2} per hour per infected cell (80). This would mean that a focus would double its size by cell-to-cell transmission (including proliferation of infected cells) in vitro within 10–24 h. The model was also used to quantify the effect of antibodies against different HCV entry receptors in inhibiting cell-to-cell spread. Despite the shortcomings of this approach, which

approximates individual irregular foci as circular ones and ignores the ongoing cell proliferation within the culture, the study provides a first estimate for HCV cell-to-cell transmission rates. It still remains to be shown how well these in vitro estimates hold in vivo.

Determining HCV spread based on viroscape profiles—Another approach to quantify HCV cell-to-cell transmission and to address transmission kinetics is based on the analysis of the viroscape profile—that is, the profile of intracellular HCV RNA levels within infected cells of different clusters. As a first step, we developed a model that uses the amount of intracellular positive-strand vRNA within infected cells, a quantity we call H, as a surrogate for the time a cell has been infected, (61, 77). The model considers the intracellular replication cycle by distinguishing between vRNA, H, and the negative strand that is part of replication complexes, R. The vRNA, H, is produced from replication complexes after a lag phase of duration a_0 and is also degraded intracellularly. Replication complexes are produced by copying vRNA at a rate that slows as the cell reaches a maximum allowed number of replication complexes, presumably due to a limitation in host cell resources. Each cell has a carrying capacity H_{max} and R_{max} of ~100 vRNAs (81) and ~40 replication complexes, respectively (81, 82). Parameterizing the model and neglecting the loss of vRNA by export within virions, the doubling time of vRNA was estimated to be ~6 h (61). Simulating the stochastic replication dynamics within a cell with such a model, and varying the lag phase between 6 and 24 h, we estimated that the cells in the liver biopsy samples might have been infected for ~5 days (3.5, 7.7) (77).

HCV viral replication and infected focus formation in a spatially explicit 2D setting can also be studied through the use of agent-based models (77). In this case, hepatocytes are modeled as cubic or hexagonal structures distributed on a regular grid (see **Figure 2**) representing a solid tissue environment or a 2D in vitro culture. Once a cell is infected, processes of intracellular viral replication are modeled as described above, distinguishing between vRNA and replication complexes. vRNA can be assembled into virions and exported from the infected cell. Extracellular virus is assumed to diffuse, and the extracellular viral concentration at different points in space is modeled (**Figure 2**). New infections occur either via cell-to-cell transmission among neighbors or via cell-free infection by diffusing virions. The rate of infection events depends on the infection probabilities for cell-to-cell and cell-free transmission, p_{cc} and p_{cf} , respectively, and on the amount of intracellular vRNA and the local extracellular viral concentration, respectively.

Such a model was used to study how the observed profile of intracellular vRNA in a cluster, the so-called viroscape, is influenced by different factors (77). The ratio of the rate at which neighboring cells become infected to the rate at which intracellular vRNA accumulates determines the steepness of the viroscape between two neighboring cells. In the liver biopsy samples analyzed by laser capture microdissection, the vRNA level within cells in the direct neighborhood of the core of a focus was only ~40% of that within the central infected cell (77). Under the assumption that the lag before the start of viral production is ~24 h, this relationship was recovered in simulations of foci spread on a 2D lattice when the probability of cell-to-cell transmission was set to $p_{cc} \approx 4 \times 10^{-2}$ per hour, which agrees with the estimates obtained for the cell-to-cell transmission rate of HCV in vitro (80).

This example nicely shows how simulation of the spatial processes involved in viral replication and spread, in combination with experimental observations, allows one to obtain estimates for the quantification of processes that are not directly observed. By varying the parameter values for p_{cc} and p_{cf} , the model of 2D HCV spread can also be used to identify the relative proportions of cell-free and cell-to-cell transmission based on the spatial pattern of infected cells at a certain time point (P. Kumberger & F. Graw, unpublished observations). Simulating these processes with a model allows one to determine how factors such as the spatial boundaries of an in vitro culture system and the merging of individual foci over time could affect the interpretation of experimental data. By combining spatially explicit mathematical models with time course data on HCV focus spread in vitro, one can quantify viral transmission modes and their impact on infection dynamics.

CONSIDERATION OF IMMUNE RESPONSES AND THE EFFECT OF TREATMENT ON VIRAL SPREAD

Analysis of clinical data on HIV-1 or HCV viral spread in vivo usually requires the consideration of the effect of antiviral treatment and potential immune responses. Mathematical modeling has helped to identify the mechanisms of action of antiviral drugs, to quantify their effectiveness, and to find appropriate doses and treatment regimens (reviewed in 33, 83). These endeavors made use of population dynamic models similar to Equation 2 that treated target cell populations, immune responses, and drug concentrations as homogeneous and well-mixed populations, appropriate to describe average dynamics. However, the increasing evidence for the importance of cell-to-cell transmission in HIV-1 and HCV in vitro and in vivo (42, 80), as well as the finding that some antiretroviral drug tissue concentrations are much lower than plasma concentrations (84) allowing viral replication and evolution (85), also demands the consideration of spatial aspects of drug efficacy and local immune responses when analyzing viral spread in vivo (**Figure 3**).

In HCV infections, the progression of infection triggers infected cells and their neighbors to start producing antiviral factors, such as type I IFN (IFN-α), which may protect uninfected cells from becoming infected and interfere with viral replication (86, 87). Thus, if viral spread mostly relies on cell-to-cell transmission, the growth of individual foci of infected cells is an arms race between the efficacy of viral spread and the local increase of antiviral factors evoked by the spread. Such a trade-off could have shaped the observed cluster profiles in HCV-infected liver tissue (77). A recent study analyzed this trade-off for dengue virus on a population level using live-cell analysis in combination with a mathematical model to study the effect on viral spread (88). Prior to that, a stochastic spatial model that included the dynamics of a type I IFN response and was parametrized by data was used to study the time-dependent spread of herpes simplex virus type 1 within a cell monolayer (89). Whether local spread can evoke local immune responses in the case of HCV still remains controversial (72, 73, 79). However, it is quite intuitive to assume that high local concentrations of virions require high antiviral drug concentrations at the same locations in order for an antiviral drug to be efficient, as has been observed for HIV-1 (12). Agent-based models can and should be used to study the kinetic relationship between viral spread and

innate immunity in a spatially confined setting to identify the relevant factors that determine disease outcome (65).

CONCLUSIONS AND FUTURE OUTLOOK

Understanding the way viruses spread in vivo is an important prerequisite to developing effective therapeutic protocols and preventive strategies. Analyzing experimental data on viral spread through the use of mathematical models should allow one to obtain a more systematic and quantitative understanding about the processes involved and to identify key targets for therapeutic interventions.

Mathematical modeling has advanced our knowledge about the kinetics of viral turnover and spread and the efficacy of drug treatment. However, modeling local spreading mechanisms, such as cell-to-cell transmission or the release of virions from one cell yielding preferential binding to neighboring cells, and the local innate responses these mechanisms may generate, requires further work.

In the light of these findings, key questions to be answered in order to understand viral dynamics and progression of infection in more detail concern (*a*) the kinetics of formation and the lifetime of cell-to-cell contacts for viral transmission, (*b*) the role of multiple viral genome transfers for persistence of infection and in reducing drug effectiveness, and (*c*) the effect of local immune responses on viral spread (**Figure 3**). Addressing these questions presents novel challenges for mathematical techniques as well as experimental methods. More complex modeling frameworks are required to capture the processes involved, and such models need corresponding support from the collection of appropriate experimental data.

Advances in experimental techniques, especially addressing the visualization of important steps of the viral life cycle and allowing live-cell imaging, have increased the possibilities to obtain the necessary quantitative data. These advances include the development of appropriate labeling techniques—for example, fluorescent tags attached to viral structural proteins, such as Gag for HIV-1 (34, 35)—that allow one to follow several rounds of replication, unlike previous techniques that were limited to a single round (62, 87, 90). In addition, a dual-color fluorescent reporter system has been developed to study how viral infections spread through a host cell monolayer and how the cellular innate immune system mounts an antiviral response (91, 92). A further improvement is the development of 3D in vitro systems to analyze viral spread in more complex environments that more closely resemble the in vivo situation (93). Live-cell imaging of viral entry on a single-cell level (94, 95); investigating viral subcellular localization and replication (74, 96); analyzing viral spread within a tissue or organism, as can be done in humanized mouse models (86); and obtaining time courses of interactions between pathogen spread and individual immune responses (97) will provide more detailed information that can be used to drive new modeling.

We are only at the beginning of using mathematical modeling as a tool to combine information from these various sources and at a various scales to generate a quantitative

understanding of viral spread. With the help of new technologies and new models we hope to understand the full dynamics of these processes in quantitative detail and to be able to identify the key processes that need to be targeted to prevent spread of infection.

ACKNOWLEDGMENTS

We thank Peter Kumberger for help with **Figure 2**. F.G. was supported by the Center for Modelling and Simulation in the Biosciences (BIOMS). Portions of this work were performed under the auspices of the US Department of Energy under contract DE-AC52-06NA25396 and supported by NIH grants R01-AI07881, R01-AI028433, R01-OD011095, and R01-AI116868 (A.S.P.).

LITERATURE CITED

1. Microbiology by numbers. Nat. Rev. Microbiol. 2011; 9:628. [PubMed: 21961177]
2. Willen, CB.; Tilton, JC.; Doms, RW. Molecular mechanisms of HIV entry. In: Rossmann, MG.; Rao, VB., editors. Viral Molecular Machines. Springer; New York: 2012.
3. Zeisel MB, Koutsoudakis G, Schnober EK, Haberstroh A, Blum HE, et al. Scavenger receptor class B type I is a key host factor for hepatitis C virus infection required for an entry step closely linked to CD81. Hepatology. 2007; 46:1722–31. [PubMed: 18000990]
4. Pileri P, Uematsu Y, Campagnoli S, Galli G, Falugi F, et al. Binding of hepatitis C virus to CD81. Science. 1998; 282:938–41. [PubMed: 9794763]
5. Evans MJ, von Hahn T, Tscherne DM, Syder AJ, Panis M, et al. Claudin-1 is a hepatitis C virus co-receptor required for a late step in entry. Nature. 2007; 446:801–5. [PubMed: 17325668]
6. Ploss A, Evans MJ, Gaysinskaya VA, Panis M, You H, et al. Human occludin is a hepatitis C virus entry factor required for infection of mouse cells. Nature. 2009; 457:882–86. [PubMed: 19182773]
7. Sainz B Jr. Barretto N, Martin DN, Hiraga N, Imamura M, et al. Identification of the Niemann-Pick C1-like 1 cholesterol absorption receptor as a new hepatitis C virus entry factor. Nat. Med. 2012; 18:281–85. [PubMed: 22231557]
8. Verrier ER, Colpitts CC, Bach C, Heydmann L, Weiss A, et al. A targeted functional RNA interference screen uncovers glypican 5 as an entry factor for hepatitis B and D viruses. Hepatology. 2016; 63:35–48. [PubMed: 26224662]
9. Yan H, Zhong G, Xu G, He W, Jing Z, et al. Sodium taurocholate cotransporting polypeptide is a functional receptor for human hepatitis B and D virus. eLife. 2012; 1:e00049. [PubMed: 23150796]
10. Martin DN, Uprichard SL. Identification of transferrin receptor 1 as a hepatitis C virus entry factor. PNAS. 2013; 110:10777–82. [PubMed: 23754414]
11. Ujino S, Nishitsuji H, Hishiki T, Sugiyama K, Takaku H, Shimotohno K. Hepatitis C virus utilizes VLDLR as a novel entry pathway. PNAS. 2016; 113:188–93. [PubMed: 26699506]
12. Sigal A, Kim JT, Balazs AB, Dekel E, Mayo A, et al. Cell-to-cell spread of HIV permits ongoing replication despite antiretroviral therapy. Nature. 2011; 477:95–98. [PubMed: 21849975]
13. Brimacombe CL, Grove J, Meredith LW, Hu K, Syder AJ, et al. Neutralizing antibody-resistant hepatitis C virus cell-to-cell transmission. J. Virol. 2011; 85:596–605. [PubMed: 20962076]
14. Abela IA, Berlinger L, Schanz M, Reynell L, Gunthard HF, et al. Cell-cell transmission enables HIV-1 to evade inhibition by potent CD4bs directed antibodies. PLOS Pathog. 2012; 8:e1002634. [PubMed: 22496655]
15. Sattentau Q. Avoiding the void: cell-to-cell spread of human viruses. Nat. Rev. Microbiol. 2008; 6:815–26. [PubMed: 18923409]
16. Mothes W, Sherer NM, Jin J, Zhong P. Virus cell-to-cell transmission. J. Virol. 2010; 84:8360–68. [PubMed: 20375157]
17. Alvarez RA, Barria MI, Chen BK. Unique features of HIV-1 spread through T cell virological synapses. PLOS Pathog. 2014; 10:e1004513. [PubMed: 25522148]
18. Chen P, Hubner W, Spinelli MA, Chen BK. Predominant mode of human immunodeficiency virus transfer between T cells is mediated by sustained Env-dependent neutralization-resistant virological synapses. J. Virol. 2007; 81:12582–95. [PubMed: 17728240]

19. Martin N, Welsch S, Jolly C, Briggs JA, Vaux D, Sattentau QJ. Virological synapse-mediated spread of human immunodeficiency virus type 1 between T cells is sensitive to entry inhibition. J. Virol. 2010; 84:3516–27. [PubMed: 20089656]
20. Sourisseau M, Sol-Foulon N, Porrot F, Blanchet F, Schwartz O. Inefficient human immunodeficiency virus replication in mobile lymphocytes. J. Virol. 2007; 81:1000–12. [PubMed: 17079292]
21. Hubner W, McNerney GP, Chen P, Dale BM, Gordon RE, et al. Quantitative 3D video microscopy of HIV transfer across T cell virological synapses. Science. 2009; 323:1743–47. [PubMed: 19325119]
22. Agosto LM, Zhong P, Munro J, Mothes W. Highly active antiretroviral therapies are effective against HIV-1 cell-to-cell transmission. PLOS Pathog. 2014; 10:e1003982. [PubMed: 24586176]
23. Agosto LM, Uchil PD, Mothes W. HIV cell-to-cell transmission: effects on pathogenesis and antiretroviral therapy. Trends Microbiol. 2015; 23:289–95. [PubMed: 25766144]
24. Komarova NL, Levy DN, Wodarz D. Synaptic transmission and the susceptibility of HIV infection to anti-viral drugs. Sci. Rep. 2013; 3:2103. [PubMed: 23811684]
25. Barretto N, Sainz B Jr. Hussain S, Uprichard SL. Determining the involvement and therapeutic implications of host cellular factors in hepatitis C virus cell-to-cell spread. J. Virol. 2014; 88:5050–61. [PubMed: 24554660]
26. Galloway NLK, Doitsh G, Monroe KM, Yang Z, Muñoz-Arias I, et al. Cell-to-cell transmission of HIV-1 is required to trigger pyroptotic death of lymphoid-tissue-derived CD4 T cells. Cell Rep. 2016; 12:1555–63.
27. Perelson AS. Modelling viral and immune system dynamics. Nat. Rev. Immunol. 2002; 2:28–36. [PubMed: 11905835]
28. Perelson AS, Neumann AU, Markowitz M, Leonard JM, Ho DD. HIV-1 dynamics in vivo: virion clearance rate, infected cell life-span, and viral generation time. Science. 1996; 271:1582–86. [PubMed: 8599114]
29. Ho DD, Neumann AU, Perelson AS, Chen W, Leonard JM, Markowitz M. Rapid turnover of plasma virions and CD4 lymphocytes in HIV-1 infection. Nature. 1995; 373:123–26. [PubMed: 7816094]
30. Neumann AU, Lam NP, Dahari H, Gretch DR, Wiley TE, et al. Hepatitis C viral dynamics in vivo and the antiviral efficacy of interferon-α therapy. Science. 1998; 282:103–7. [PubMed: 9756471]
31. Ramratnam B, Bonhoeffer S, Binley J, Hurley A, Zhang L, et al. Rapid production and clearance of HIV-1 and hepatitis C virus assessed by large volume plasma apheresis. Lancet. 1999; 354:1782–85. [PubMed: 10577640]
32. Guedj J, Dahari H, Rong L, Sansone ND, Nettles RE, et al. Modeling shows that the NS5A inhibitor daclatasvir has two modes of action and yields a shorter estimate of the hepatitis C virus half-life. PNAS. 2013; 110:3991–96. [PubMed: 23431163]
33. Chatterjee A, Guedj J, Perelson AS. Mathematical modelling of HCV infection: What can it teach us in the era of direct-acting antiviral agents? Antivir. Ther. 2012; 17:1171–82. [PubMed: 23186606]
34. Dixit NM, Layden-Almer JE, Layden TJ, Perelson AS. Modelling how ribavirin improves interferon response rates in hepatitis C virus infection. Nature. 2004; 432:922–24. [PubMed: 15602565]
35. Guedj J, Dahari H, Pohl RT, Ferenci P, Perelson AS. Understanding silibinin's modes of action against HCV using viral kinetic modeling. J. Hepatol. 2012; 56:1019–24. [PubMed: 22245888]
36. Perelson, AS. Mathematical modeling. In: Katze, MG.; Korth, MJ.; Law, GL.; Nathanson, N., editors. Viral Pathogenesis: From Basics to Systems Biology. Academic; Amsterdam: 2016. p. 199-211.
37. Nowak, M.; May, R. Virus Dynamics: Mathematical Principles of Immunology and Virology. Oxford Univ. Press; Oxford, UK: 2000.
38. Perelson AS, Ribeiro RM. Modeling the within-host dynamics of HIV infection. BMC Biol. 2013; 11:96. [PubMed: 24020860]

39. Zhang C, Zhou S, Groppelli E, Pellegrino P, Williams I, et al. Hybrid spreading mechanisms and T cell activation shape the dynamics of HIV-1 infection. PLOS Comput. Biol. 2015; 11:e1004179. [PubMed: 25837979]
40. Komarova NL, Levy DN, Wodarz D. Effect of synaptic transmission on viral fitness in HIV infection. PLOS ONE. 2012; 7:e48361. [PubMed: 23166585]
41. Komarova NL, Wodarz D. Virus dynamics in the presence of synaptic transmission. Math. Biosci. 2013; 242:161–71. [PubMed: 23357287]
42. Iwami S, Takeuchi JS, Nakaoka S, Mammano F, Clavel F, et al. Cell-to-cell infection by HIV contributes over half of virus infection. eLife. 2015; 4:e08150.
43. Murooka TT, Deruaz M, Marangoni F, Vrbanac VD, Seung E, et al. HIV-infected T cells are migratory vehicles for viral dissemination. Nature. 2012; 490:283–87. [PubMed: 22854780]
44. Dixit NM, Perelson AS. Multiplicity of human immunodeficiency virus infections in lymphoid tissue. J. Virol. 2004; 78:8942–45. [PubMed: 15280505]
45. Vasiliver-Shamis G, Dustin ML, Hioe CE. HIV-1 virological synapse is not simply a copycat of the immunological synapse. Viruses. 2010; 2:1239–60. [PubMed: 20890395]
46. Jolly C, Kashefi K, Hollinshead M, Sattentau QJ. HIV-1 cell to cell transfer across an Env-induced, actin-dependent synapse. J. Exp. Med. 2004; 199:283–93. [PubMed: 14734528]
47. Jolly C, Mitar I, Sattentau QJ. Adhesion molecule interactions facilitate human immunodeficiency virus type 1-induced virological synapse formation between T cells. J. Virol. 2007; 81:13916–21. [PubMed: 17913807]
48. Rudnicka D, Feldmann J, Porrot F, Wietgrefe S, Guadagnini S, et al. Simultaneous cell-to-cell transmission of human immunodeficiency virus to multiple targets through polysynapses. J. Virol. 2009; 83:6234–46. [PubMed: 19369333]
49. Vasiliver-Shamis G, Tuen M, Wu TW, Starr T, Cameron TO, et al. Human immunodeficiency virus type 1 envelope gp120 induces a stop signal and virological synapse formation in noninfected $CD4^+$ T cells. J. Virol. 2008; 82:9445–57. [PubMed: 18632854]
50. McDonald D, Wu L, Bohks SM, KewalRamani VN, Unutmaz D, Hope TJ. Recruitment of HIV and its receptors to dendritic cell-T cell junctions. Science. 2003; 300:1295–97. [PubMed: 12730499]
51. Cameron PU, Freudenthal PS, Barker JM, Gezelter S, Inaba K, Steinman RM. Dendritic cells exposed to human immunodeficiency virus type-1 transmit a vigorous cytopathic infection to $CD4^+$ T cells. Science. 1992; 257:383–87. [PubMed: 1352913]
52. Brandenberg OF, Magnus C, Regoes RR, Trkola A. The HIV-1 entry process: a stoichiometric view. Trends Microbiol. 2015; 23:763–74. [PubMed: 26541228]
53. Del Portillo A, Tripodi J, Najfeld V, Wodarz D, Levy DN, Chen BK. Multiploid inheritance of HIV-1 during cell-to-cell infection. J. Virol. 2011; 85:7169–76. [PubMed: 21543479]
54. Russell RA, Martin N, Mitar I, Jones E, Sattentau QJ. Multiple proviral integration events after virological synapse-mediated HIV-1 spread. Virology. 2013; 443:143–49. [PubMed: 23722103]
55. Jung A, Maier R, Vartanian JP, Bocharov G, Jung V, et al. Recombination: multiply infected spleen cells in HIV patients. Nature. 2002; 418:144. [PubMed: 12110879]
56. Josefsson L, King MS, Makitalo B, Brannstrom J, Shao W, et al. Majority of $CD4^+$ T cells from peripheral blood of HIV-1-infected individuals contain only one HIV DNA molecule. PNAS. 2011; 108:11199–204. [PubMed: 21690402]
57. Piguet V, Gu F, Foti M, Demaurex N, Gruenberg J, et al. Nef-induced CD4 degradation: A diacidic-based motif in Nef functions as a lysosomal targeting signal through the binding of β-COP in endosomes. Cell. 1999; 97:63–73. [PubMed: 10199403]
58. Miyashita S, Ishibashi K, Kishino H, Ishikawa M. Viruses roll the dice: The stochastic behavior of viral genome molecules accelerates viral adaptation at the cell and tissue levels. PLOS Biol. 2015; 13:e1002094. [PubMed: 25781391]
59. Richardson LA. Viral cell-to-cell transmission—why less is more. PLOS Biol. 2015; 13:e1002095. [PubMed: 25781563]
60. Guedj J, Pang PS, Denning J, Rodriguez-Torres M, Lawitz E, et al. Analysis of hepatitis C viral kinetics during administration of two nucleotide analogues: sofosbuvir (GS-7977) and GS-0938. Antivir. Ther. 2014; 19:211–20. [PubMed: 24464551]

61. Ribeiro RM, Li H, Wang S, Stoddard MB, Learn GH, et al. Quantifying the diversification of hepatitis C virus (HCV) during primary infection: estimates of the in vivo mutation rate. PLOS Pathog. 2012; 8:e1002881. [PubMed: 22927817]
62. Rong L, Dahari H, Ribeiro RM, Perelson AS. Rapid emergence of protease inhibitor resistance in hepatitis C virus. Sci. Transl. Med. 2010; 2:30ra32.
63. Perelson AS, Guedj J. Modelling hepatitis C therapy—predicting effects of treatment. Nat. Rev. Gastroenterol. Hepatol. 2015; 12:437–45. [PubMed: 26122475]
64. Lau G, Benhamou Y, Chen G, Li J, Shao Q, et al. Efficacy and safety of three week response-guided direct-acting antiviral therapy: a phase 2, proof-of-concept study. Lancet Gastroenterol. Hepatol. 2016 In press.
65. Bauer AL, Beauchemin CA, Perelson AS. Agent-based modeling of host-pathogen systems: the successes and challenges. Inf. Sci. 2009; 179:1379–89.
66. Beauchemin C, Samuel J, Tuszynski J. A simple cellular automaton model for influenza A viral infections. J. Theor. Biol. 2005; 232:223–34. [PubMed: 15530492]
67. Zorzenon dos Santos RM, Coutinho S. Dynamics of HIV infection: a cellular automata approach. Phys. Rev. Lett. 2001; 87:168102. [PubMed: 11690248]
68. Funk GA, Jansen VA, Bonhoeffer S, Killingback T. Spatial models of virus-immune dynamics. J. Theor. Biol. 2005; 233:221–36. [PubMed: 15619362]
69. Frank SA. Within-host spatial dynamics of viruses and defective interfering particles. J. Theor. Biol. 2000; 206:279–90. [PubMed: 10966764]
70. Graziano FM, Kettoola SY, Munshower JM, Stapleton JT, Towfic GJ. Effect of spatial distribution of T-cells and HIV load on HIV progression. Bioinformatics. 2008; 24:855–60. [PubMed: 18187444]
71. Strain MC, Richman DD, Wong JK, Levine H. Spatiotemporal dynamics of HIV propagation. J. Theor. Biol. 2002; 218:85–96. [PubMed: 12297072]
72. Kandathil AJ, Graw F, Quinn J, Hwang HS, Torbenson M, et al. Use of laser capture microdissection to map hepatitis C virus-positive hepatocytes in human liver. Gastroenterology. 2013; 145:1404–13. [PubMed: 23973767]
73. Wieland S, Makowska Z, Campana B, Calabrese D, Dill MT, et al. Simultaneous detection of hepatitis C virus and interferon stimulated gene expression in infected human liver. Hepatology. 2014; 59:2121–30. [PubMed: 24122862]
74. Shulla A, Randall G. Spatiotemporal analysis of hepatitis C virus infection. PLOS Pathog. 2015; 11:e1004758. [PubMed: 25822891]
75. Binder M, Sulaimanov N, Clausznitzer D, Schulze M, Huber CM, et al. Replication vesicles are load- and choke-points in the hepatitis C virus lifecycle. PLOS Pathog. 2013; 9:e1003561. [PubMed: 23990783]
76. Dahari H, Ribeiro RM, Rice CM, Perelson AS. Mathematical modeling of subgenomic hepatitis C virus replication in Huh-7 cells. J. Virol. 2007; 81:750–60. [PubMed: 17035310]
77. Graw F, Balagopal A, Kandathil AJ, Ray SC, Thomas DL, et al. Inferring viral dynamics in chronically HCV infected patients from the spatial distribution of infected hepatocytes. PLOS Comput. Biol. 2014; 10:e1003934. [PubMed: 25393308]
78. Liang Y, Shilagard T, Xiao SY, Snyder N, Lau D, et al. Visualizing hepatitis C virus infections in human liver by two-photon microscopy. Gastroenterology. 2009; 137:1448–58. [PubMed: 19632233]
79. Stiffler JD, Nguyen M, Sohn JA, Liu C, Kaplan D, Seeger C. Focal distribution of hepatitis C virus RNA in infected livers. PLOS ONE. 2009; 4:e6661. [PubMed: 19688046]
80. Graw F, Martin DN, Perelson AS, Uprichard SL, Dahari H. Quantification of hepatitis C virus cell-to-cell spread using a stochastic modeling approach. J. Virol. 2015; 89:6551–61. [PubMed: 25833046]
81. Quinkert D, Bartenschlager R, Lohmann V. Quantitative analysis of the hepatitis C virus replication complex. J. Virol. 2005; 79:13594–605. [PubMed: 16227280]
82. Chang M, Williams O, Mittler J, Quintanilla A, Carithers RL Jr. et al. Dynamics of hepatitis C virus replication in human liver. Am. J. Pathol. 2003; 163:433–44. [PubMed: 12875965]

83. Canini L, Perelson AS. Viral kinetic modeling: state of the art. J. Pharmacokinet. Pharmacodyn. 2014; 41:431–43. [PubMed: 24961742]
84. Fletcher CV, Staskus K, Wietgrefe S, Bedford T, Rotherberger M, et al. Persistent HIV-1 replication is associated with lower antiretroviral drug concentrations in lymphatic tissues. PNAS. 2015; 111:2307–12.
85. Lorenzo-Redondo R, Fryer HR, Bedford T, Kim EY, Archer J, et al. Persistent HIV-1 replication maintains the tissue reservoir during therapy. Nature. 2016; 530:51–56. [PubMed: 26814962]
86. Metz P, Dazert E, Ruggieri A, Mazur J, Kaderali L, et al. Identification of type I and type II interferon-induced effectors controlling hepatitis C virus replication. Hepatology. 2012; 56:2082–93. [PubMed: 22711689]
87. Takahashi K, Asabe S, Wieland S, Garaigorta U, Gastaminza P, et al. Plasmacytoid dendritic cells sense hepatitis C virus-infected cells, produce interferon, and inhibit infection. PNAS. 2010; 107:7431–36. [PubMed: 20231459]
88. Schmid B, Rinas M, Ruggieri A, Acosta EG, Bartenschlager M, et al. Live cell analysis and mathematical modeling identify determinants of attenuation of dengue virus $2^{\pm}$-O-methylation mutant. PLOS Pathog. 2015; 11:e1005345. [PubMed: 26720415]
89. Howat TJ, Barreca C, O'Hare P, Gog JR, Grenfell BT. Modelling dynamics of the type I interferon response to in vitro viral infection. J. R. Soc. Interface. 2006; 3:699–709. [PubMed: 16971338]
90. McDonald D, Vodicka MA, Lucero G, Svitkina TM, Borisy GG, et al. Visualization of the intracellular behavior of HIV in living cells. J. Cell Biol. 2002; 159:441–52. [PubMed: 12417576]
91. Swick A, Baltes A, Yin J. Visualizing infection spread: dual-color fluorescent reporting of virus-host interactions. Biotechnol. Bioeng. 2014; 111:1200–9. [PubMed: 24338628]
92. Voigt EA, Swick A, Yin J. Rapid induction and persistence of paracrine-induced cellular antiviral states arrest viral infection spread in A549 cells. Virology. 2016 In press.
93. Fackler OT, Murooka TT, Imle A, Mempel TR. Adding new dimensions: towards an integrative understanding of HIV-1 spread. Nat. Rev. Microbiol. 2014; 12:563–74. [PubMed: 25029025]
94. Dinh MH, Anderson MR, McRaven MD, Cianci GC, McCoombe SG, et al. Visualization of HIV-1 interactions with penile and foreskin epithelia: clues for female-to-male HIV transmission. PLOS Pathog. 2015; 11:e1004729. [PubMed: 25748093]
95. Koch P, Lampe M, Godinez WJ, Muller B, Rohr K, et al. Visualizing fusion of pseudotyped HIV-1 particles in real time by live cell microscopy. Retrovirology. 2009; 6:84. [PubMed: 19765276]
96. Di Primio C, Quercioli V, Allouch A, Gijsbers R, Christ F, et al. Single-cell imaging of HIV-1 provirus (SCIP). PNAS. 2013; 110:5636–41. [PubMed: 23513220]
97. Coombes JL, Robey EA. Dynamic imaging of host-pathogen interactions in vivo. Nat. Rev. Immunol. 2010; 10:353–64. [PubMed: 20395980]

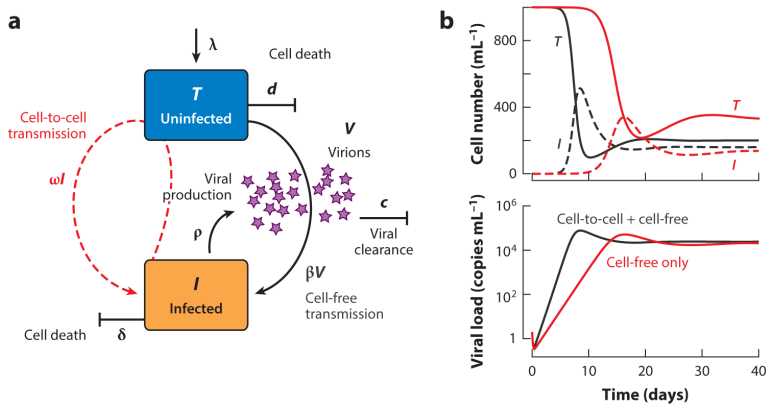

Figure 1.

(*a*) Sketch of the mathematical model given by Equation 1, describing viral spread by cell-to-cell (*red*) and cell-free (*black*) transmission. (*b*) Dynamics of uninfected (*solid line*) and infected (*dashed line*) cells (*upper panel*), and corresponding dynamics of cell-free virus (*lower panel*), for realizations of the model allowing for either cell-to-cell and cell-free transmission (*black*) or only cell-free transmission (*red*). Parameters used in the model were $\lambda = 100\ \text{day}^{-1}$, $d = 0.1\ \text{day}^{-1}$, $\rho = 1.5 \times 10^{3}\ \text{day}^{-1}$, $c = 10\ \text{day}^{-1}$, $\delta = 0.5\ \text{day}^{-1}$, $\beta = 10^{-5}$ day^{-1} per virion, and $\omega = 10^{-3}\ \text{day}^{-1}$ per infected cell.

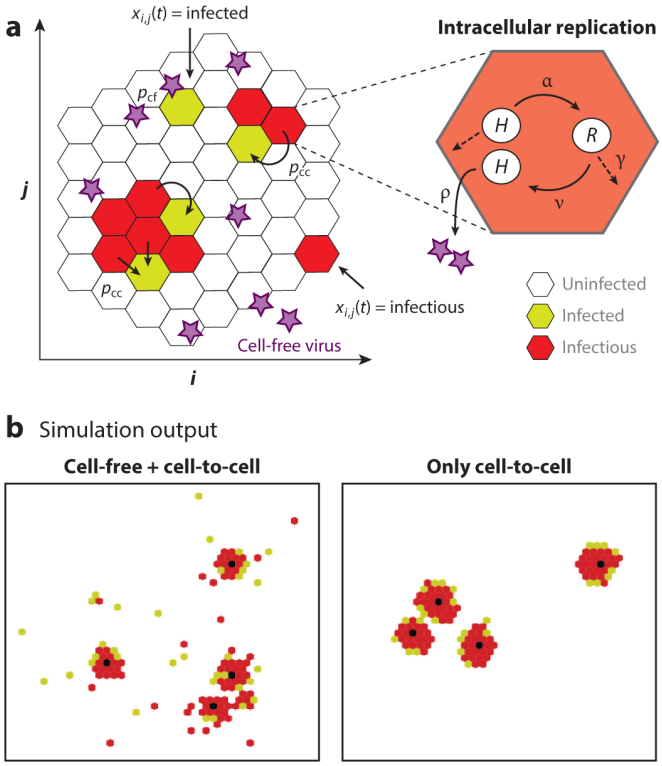

Figure 2.

Agent-based model of hepatitis C virus cell-to-cell spread. (*a*) Cells are modeled as hexagonal structures within a regular grid and can change their status, $x_{i,j}(t)$, with time. Uninfected cells (*white hexagons*) get infected (*green hexagons*) by cell-free virus (*purple stars*) with probability p_{cf} or by cell-to-cell transmission from direct neighbors that are infectious (*red hexagons*) with probability p_{cc}. Intracellular viral replication and viral export are explicitly modeled, distinguishing between positive-strand vRNA (*H*) and replication complexes (*R*). Positive-strand vRNA is responsible for cell-to-cell transmission and, when exported in viral particles, for cell-free virus transmission. Cell-free virus can diffuse throughout the grid. Infection is initiated by introducing a limited number of infected cells onto the grid. (*b*) Output from two simulations assuming either cell-free and cell-to-cell transmission (*left*) or only cell-to-cell transmission (*right*). Simulations comprise ~10,000 cells in total, and snapshots of parts of the simulated cell culture are shown when a total of ~300 cells were infected. The black hexagons indicate the initially infected cell that founded the corresponding large infected cell focus.

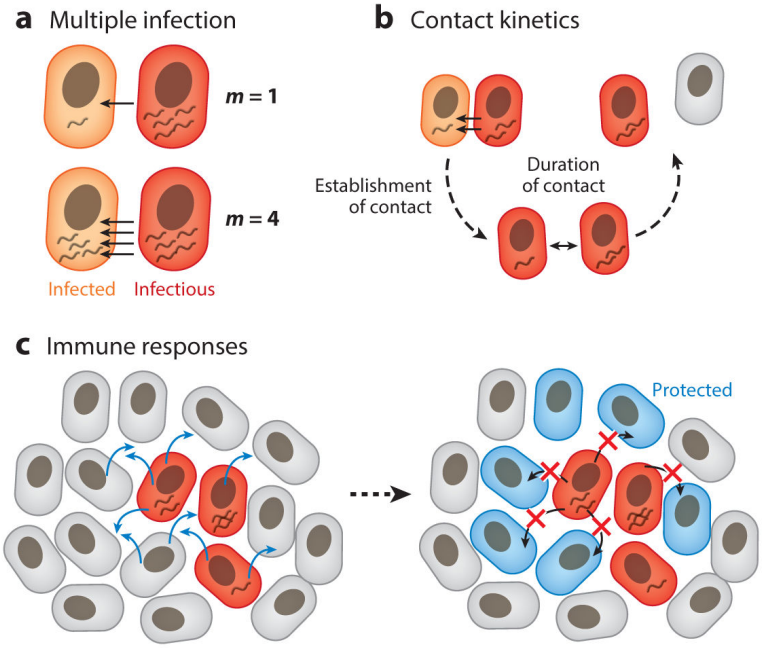

Figure 3.

Current challenges for the analysis of viral spread. (*a*) The number of viral particles transmitted per contact, *m*, and how the magnitude of *m* affects viral dynamics and evolution are not known. (*b*) The kinetics of contact formation and duration of contact needed to successfully infect other cells are also not known in the case of motile cells, such as $CD4^+$ T cells. (*c*) The dynamics and protective capacity of local innate immune responses triggered by infection, such as type I interferon (IFN) responses, still need to be characterized for most viral infections. How quickly agents such as IFN released by infected and nearby cells (e.g., plasmacytoid dendritic cells or target cells in which viral products have been sensed but that have not yet become productively infected) render neighboring cells protected against infection is still an open question. Quantification of these processes is needed in order to advance the analysis of viral spread. Red cells are infectious, orange cells are becoming infected, blue cells are protected, and gray cells are uninfected. Blue arrows indicate release of IFN, and black arrows with red crosses indicate the spread of infection being blocked due to the protected state of blue cells.